

## Development of a Hydraulic Solver for the Safety Analysis Codes for Nuclear Power Plants(I)

*S. Y Lee, J. C. Park, M. T. Oh, S. C. Moon, and C. E. Park*

*Korea Power Engineering Company, Inc., 150 Deokjin-dong, Yuseong-gu, Daejeon, 305-353*

### 1. Introduction

In this study, a three-field pilot code is developed for a one-dimensional channel flow based on the reference[1]. The three fields are comprised of a gas, continuous liquid and entrained liquid fields. Unlike the study in the reference[1], the temperatures of continuous liquid and entrained liquid are assumed to be non-equilibrium. Other noticeable difference is to adopt the phase temperatures as primitive variables. Using ten conceptual problems, the pilot code has been verified. Special attention has been paid on the verification of the behavior of the noncondensable gas phase.

### 2. Main Features

#### 2.1 Governing equations

The present one-dimensional thermal hydraulic pilot code model solves ten governing equations using the semi-implicit scheme. The primitive unknown variables are chosen to be noncondensable gas pressure( $P_n$ ), phasic temperatures( $T_v, T_d, T_l$ ), phasic volume fractions ( $\alpha_v, \alpha_d$ ), total pressure( $P$ ), and phasic velocities ( $u_v, u_l, u_d$ ).

##### 2.1.1 Continuity equations

$$\begin{aligned} \frac{\partial}{\partial t}(\alpha_v \rho_v) + \frac{1}{A} \frac{\partial}{\partial x}(\alpha_v \rho_v u_v A) &= \Gamma_l + \Gamma_d \\ \frac{\partial}{\partial t}(\alpha_l \rho_l) + \frac{1}{A} \frac{\partial}{\partial x}(\alpha_l \rho_l u_l A) &= -\Gamma_l - S_E + S_D \\ \frac{\partial}{\partial t}(\alpha_d \rho_d) + \frac{1}{A} \frac{\partial}{\partial x}(\alpha_d \rho_d u_d A) &= -\Gamma_d + S_E - S_D \\ \frac{\partial}{\partial t}(\alpha_n \rho_n) + \frac{1}{A} \frac{\partial}{\partial x}(\alpha_n \rho_n u_n A) &= 0 \end{aligned}$$

The interfacial mass transfer is divided into the mass transfer ( $\Gamma_l$ ) at the vapor/liquid interface and the mass transfer ( $\Gamma_d$ ) at the vapor/droplet interface.

##### 2.1.2 Momentum equations

$$\begin{aligned} \alpha_g(\rho_v + \rho_n) \frac{\partial u_v}{\partial t} + \alpha_g(\rho_v + \rho_n) u_v \frac{\partial u_v}{\partial x} &= -\alpha_g \frac{\partial P}{\partial x} \\ + \alpha_g(\rho_v + \rho_n) B_x - F_{vv}(u_v) - F_{vd}(u_v - u_d) - F_{vl}(u_v - u_l) \\ + \Gamma_{l,E} u_l + \Gamma_{d,E} u_d - \Gamma_{l,E} u_v - \Gamma_{d,E} u_v \\ - C_{v,vd} \alpha_v \alpha_d \rho_{m,vd} \frac{\partial(u_v - u_d)}{\partial t} - C_{v,vl} \alpha_v \alpha_l \rho_{m,vl} \frac{\partial(u_v - u_l)}{\partial t} \end{aligned}$$

$$\begin{aligned} \alpha_l \rho_l \frac{\partial u_l}{\partial t} + \alpha_l \rho_l u_l \frac{\partial u_l}{\partial x} &= -\alpha_l \frac{\partial P}{\partial x} + \alpha_l \rho_l B_x \\ - F_{vl}(u_l) - F_{lv}(u_l - u_v) + S_D u_d \\ - \Gamma_{l,C} u_l + \Gamma_{l,C} u_v - u_l S_D - C_{v,lv} \alpha_l \alpha_v \rho_{m,lv} \frac{\partial(u_l - u_v)}{\partial t} \\ \alpha_d \rho_d \frac{\partial u_d}{\partial t} + \alpha_d \rho_d u_d \frac{\partial u_d}{\partial x} &= -\alpha_d \frac{\partial P}{\partial x} + \alpha_d \rho_d B_x \\ - F_{vd}(u_d) - F_{dv}(u_d - u_v) + S_E u_l \\ - \Gamma_{d,C} u_d + \Gamma_{d,C} u_v - u_d S_E - C_{v,dv} \alpha_d \alpha_v \rho_{m,dv} \frac{\partial(u_d - u_v)}{\partial t} \end{aligned}$$

The phasic momentum equations are used in an expanded form. These equations have the pressure gradient, the body force, interface frictional drag, wall friction, interfacial mass transfer, and virtual mass term.

##### 2.1.3 Energy equations

$$\begin{aligned} \frac{\partial(\alpha_g(\rho_v e_v + \rho_n e_n))}{\partial t} + \left(\frac{1}{A}\right) \frac{\partial(A \alpha_v u_v (\rho_v e_v + \rho_n e_n))}{\partial x} &= -P \frac{\partial \alpha_g}{\partial t} \\ - \left(\frac{P}{A}\right) \frac{\partial(A \alpha_g u_v)}{\partial x} + Q_{iv-l} + \Gamma_l h_{vl}^* + \Gamma_d h_{vd}^* + Q_{iv-d} + Q_{l-n} + Q_{d-n} \\ \frac{\partial(\alpha_l \rho_l e_l)}{\partial t} + \left(\frac{1}{A}\right) \frac{\partial(A \alpha_l \rho_l e_l u_l)}{\partial x} &= -P \frac{\partial \alpha_l}{\partial t} - \left(\frac{P}{A}\right) \frac{\partial(A \alpha_l u_l)}{\partial x} \\ + Q_{il} - \Gamma_l h_l^* - S_E h_l + S_D h_d - Q_{l-n} \\ \frac{\partial(\alpha_d \rho_d e_d)}{\partial t} + \left(\frac{1}{A}\right) \frac{\partial(A \alpha_d \rho_d e_d u_d)}{\partial x} &= -P \frac{\partial \alpha_d}{\partial t} - \left(\frac{P}{A}\right) \frac{\partial(A \alpha_d u_d)}{\partial x} \\ + Q_{id} - \Gamma_d h_d^* + S_E h_l - S_D h_d - Q_{d-n} \end{aligned}$$

The vapor/non-condensable gas is assumed to be at the thermal equilibrium state but separate energy equations are set up both for liquid and droplet fields.

#### 2.2 Integrity of the equations during appearance and/or disappearance of a phase

When a phase disappears in a certain control volume during time advancement, the system of equations becomes singular. In order to avoid the singularity, a large value( $10^6$ ) of the interfacial heat transfer coefficient for the depleted phase is used instead of zero. This results in the temperature of that phase being computed very close to saturation conditions. And the phasic energy, density of the missing phase and its derivatives with respect to the pressure and temperature are calculated to the saturation values in the state relations subroutine. On the other hand,

the interfacial heat transfer coefficient associated with the mass transfer from the absent phase, is reset to zero(see Table 1).

Table 1 Interfacial heat transfer coefficient at the singular condition

| State of the fluid flow                 | Hivl                   | Hivd                   | Hil                    | Hid    | Hln | Hdn | Hld    |
|---|------------------------|------------------------|------------------------|--------|-----|-----|--------|
| $\alpha_v = 0$<br>( $\alpha_d = 0$ )    | $10^6$                 | 0                      | 0<br>If<br>$T_l < T_s$ | 0      | 0   | 0   | $10^6$ |
| $\alpha_d = 0$<br>( $\alpha_v \neq 0$ ) | -                      | 0<br>If<br>$T_v > T_s$ | -                      | $10^6$ | -   | 0   | 0      |
| $\alpha_l = 0$                          | 0<br>If<br>$T_v > T_s$ | -                      | $10^6$                 | -      | 0   | -   | 0      |

\*Hivl: Heat transfer coefficient between liquid-vapor interface and vapor  
 Hivd: Heat transfer coefficient between drop-vapor interface and vapor  
 Hil: Heat transfer coefficient between liquid-vapor interface and liquid  
 Hid: Heat transfer coefficient between drop-vapor interface and drop  
 Hln: Heat transfer coefficient between liquid and noncondensable gas  
 Hdn: Heat transfer coefficient between drop and noncondensable gas  
 Hld: Artificial heat transfer coefficient between liquid and drop, always zero

except when  $\alpha_v = 0$ , and  $\alpha_d = 0$

### 3. Test results

#### 3.1 Manometer test

Nitrogen-water manometer was set up to check the code integrity including the noncondensable gas model. The first 10 volumes were oriented vertically downward and the last 10 volumes were oriented vertically upward. To initiate the oscillation by head difference, the bottom two volumes on the left hand side and the bottom eight volumes on the right hand side were filled with water at 100.11kPa and 323K. The remaining volumes were initialized with dry nitrogen at the same pressure and temperature. The liquid oscillates back and forth between the two vertical columns with decreasing amplitude due to wall friction. The calculated period of oscillation by the code is shown to be about 4.5 seconds, which agrees well with the theoretical value, 4.486.

#### 3.2 Spray test

In this test, 20 vertical volumes were initially filled with saturated vapor at 1000 kPa. The subcooled droplet(441 K) was injected at the flowrate, 0.1 kg/s, through the uppermost junction from 5 to 50 seconds.

As shown in Figure 2, liquid field has higher temperature than droplet, since the liquid field has relatively small fraction compared with the droplet field in the test volume. The droplet energy equation is expected to be helpful to analyze more realistically such situation as pressurizer spray flow, where thermal hydraulic behavior of droplet field is not much dependent on the continuous liquid.

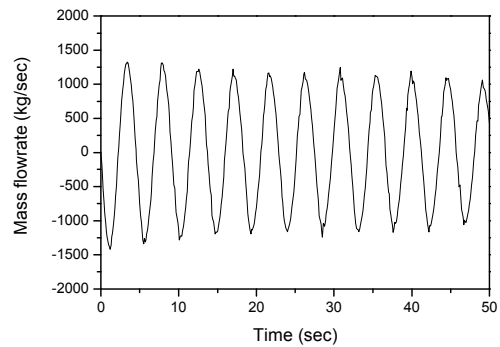


Figure 1 Mass flowrate at the bottom of the manometer

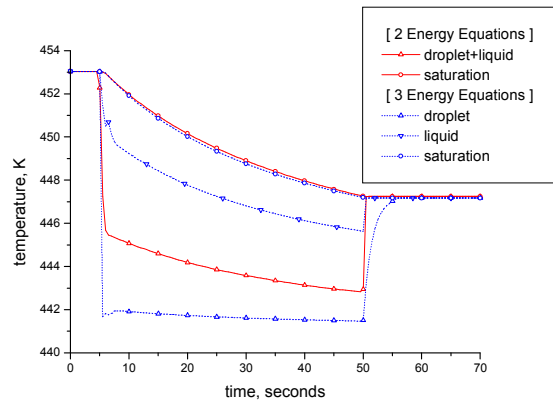


Figure 2 Temperature behavior of the droplet and continuous liquid at the uppermost node.

### 4. Conclusion

Following confirmations are obtained through this study. First, the adoption of the temperatures as primitive variables was successful. The conservation equation for noncondensable gas phase is properly working. Thermal non-equilibrium between the dispersed liquid phase and continuous liquid phase can be properly treated by using two independent liquid energy equations.

### Acknowledgment

This study was performed under the project, "Development of safety analysis codes for nuclear power plants" sponsored by the Ministry of Commerce, Industry and Energy.

### REFERENCES

- [1] Development and verification of a pilot Code Base on Two-fluid Three-field Model. Sep. 12, 2006, KAERI/TR-3239